(A New Proposal to Jefferson Lab PAC-50)

Measurement of the Beam Normal Single Spin Asymmetry in Deep Inelastic Scattering using the SoLID Spectrometer

Spokespeople: Michael Nycz[1a], William Henry[b], Ye Tian[c], Weizhi Xiong[c], Xiaochao Zheng[a]

[a]*University of Virginia, Charlottesville, Virginia 22904, USA*

[b]*Thomas Jefferson National Accelerator Facility, Newport News, Virginia 23606, USA*

[c]*Syracuse University, Syracuse, NY 13244, USA*

(Jefferson Lab SoLID and Hall A Collaborations [2])

May 15, 2022

Executive Summary

We propose a measurement of the beam-normal single-spin asymmetry A_n of the proton in the deep inelastic scattering (DIS) regime. We will use the electron beam of CEBAF, with the electron spin polarized in the transverse direction, incident on a 40-cm long liquid hydrogen target. Scattered electrons will be detected in the SoLID spectrometer in Hall A of JLab in its PVDIS configuration, with scattering angle between $\theta = (22^\circ, 35^\circ)$ and a full azimuthal angle (ϕ) coverage. By flipping the electron spin direction between (pointing) beam-left and beam-right or between vertical up and down, the beam-normal asymmetry A_n will be determined by the ϕ-dependence of the measured asymmetry.

In the Born approximation, in which a single photon is exchanged, Single Spin Normal Asymmetries (SSNA) – with either the electron (BNSSA) or the hadron target (TNSSA) spin polarized transverse to the scattering plane – are strictly forbidden due to time-reversal and parity invariance. Going beyond the Born approximation, one finds non-zero SSNA due to two-photon exchange, and effects beyond the parton-model may enhance such asymmetry. Previous measurements of PVES in the elastic region showed large A_n asymmetry, but the 6 GeV PVDIS experiment at JLab revealed A_n in DIS to be consistent with zero albeit with large statistical uncertainty. Therefore, the proposed measurement will investigate, for the first time to a high precision, the effect of two-photon exchange in DIS via BNSSA and possible effects beyond the parton-model description that may enhance the asymmetry.

We request 38 PAC days of beam time that includes 4 days of commissioning and calibration or systematic studies and 4 days for the beam polarimetry measurement. The production beam time will utilize transversely polarized beam at 70μA and includes 17 days at 6.6 GeV and 13 days at 11 GeV. By fitting the ϕ-dependence of the measured asymmetry, we will reach a precision of a few parts per million (ppm) per each 1 GeV^2-wide Q^2 bin of DIS. If combining all Q^2 bins, the combined precision on A_n can reach about ± 2.1 ppm for the 6.6 GeV and ± 3.8 ppm for the 11 GeV setting. Results from this measurement will provide the first high-precision test of two photon exchange calculation on BNSSA in the DIS region. If the asymmetry is enhanced by any effect beyond the parton model, we will be able to reveal it.

[1]Contact Person, email: mnycz@jlab.org

[2]For full author list please see SoLID Collaboration list and Hall A Collaboration list

Contents

1 Introduction

1.1 Two Photon Exchange Physics

Our understanding and description of the internal structure of both nuclei and nucleons have seen a steady improvement over the past several decades. These improvements are sometimes brought on by inconsistent or unexplained experimental results, revealing limitations of our underlying assumptions. One such example is that of the discrepancy in the extraction of G_E^p/G_M^p, the ratio of the proton form factors of elastic scattering from either Rosenbluth or polarization transfer measurements at large Q^2, see e.g. [1] and references therein. At present, this discrepancy is attributed to two-photon exchange (TPE) and is used to quantify such effect [2].

With a focus on high precision measurements in future experiments, it is vital to expand on our understanding of these higher order processes. A renewed interest in interactions beyond the Born or single-photon exchange approximation has persisted, with a number of experiments over the recent years to study the effect, but most are focusing on the elastic regime. For example, comparison of electron vs. positron elastic scattering off the proton has been made at the VEPP-3 Storage Ring [3], using CLAS [4] at JLab, and by the OLYMPUS experiment at DESY [5]. Studies of TPE also form part of the main thrust of a potential positron program at JLab [6], with some ideas focusing on the use of small-acceptance spectrometers [7, 8, 9] while others using CLAS12 [10]. However, a precision comparison between electron and positron scattering has its own challenges with one of the main systematic uncertainties being the relative luminosity control between the two beams. For example, OLYMPUS reached a 0.36% uncertainty in the e^+ vs. e^- relative luminosity difference, a significant accomplishment yet large compared with the expected size of TPE for the Q^2 range of the experiment. The goal of the proposed measurement is to study TPE and other higher-order effects by measuring the beam-normal single-spin asymmetry to a high precision in the deep inelastic scattering (DIS) regime, and has different systematic uncertainties from experiments utilizing the positrons.

1.2 Single Spin Normal Asymmetry

One way that TPE effects have been investigated is through measurements of single spin asymmetries where either the lepton (incoming or outgoing) or the target spin is polarized normal to the scattering plane, i.e., polarized along $\vec{k} \times \vec{k}'$ with $\vec{k}$ and $\vec{k}'$ the incoming and scattered electron's momentum, respectively. At the Born level, in which a single photon is exchanged, Single-Spin Normal Asymmetries (SSNAs) are forbidden due to time-reversal invariance as well as parity conservation [11]. Going beyond the Born approximation, SSNAs are no longer restricted and can provide direct access and insight into TPE effects. Figure 1 illustrates the single and two photon exchange processes, and the interference between their amplitudes results in the SSNAs.

There are two types of SSNAs that can be readily measured experimentally: Beam-Normal SSA (BNSSA) where the initial beam is polarized and the target is unpolarized, or Target-Normal SSA (TNSSA) where the beam is unpolarized and the target is polarized. SSNAs can also be studied by measuring the spin polarization of the scattered lepton or of the final-state hadronic system, but these are much harder to access experimentally and we do not discuss them here.

For electrons polarized normal to the scattering plane which interact with an unpolarized target, the BNSSA can be described as [12]:

$$A_{\mathrm{n}} = \frac{\sigma^{\uparrow} - \sigma^{\downarrow}}{\sigma^{\uparrow} + \sigma^{\downarrow}} \propto \frac{\alpha_{em} m_e}{Q} \epsilon_{\gamma\delta\lambda\mu} S^{\gamma} P^{\delta} k^{\lambda} k'^{\mu} \tag{1}$$

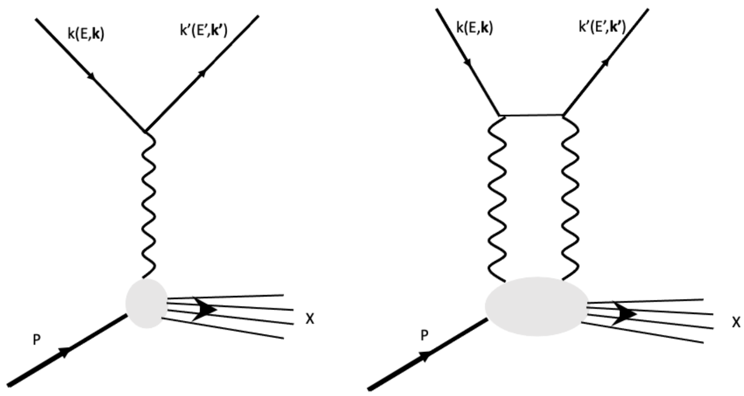

Figure 1: Feynman diagram for one (left) and two (right) photon exchange processes. The single spin asymmetries are due to the interference between the two amplitudes.

where $\sigma^{\uparrow}$ and $\sigma^{\downarrow}$ refer to the cross sections of spin up and spin down electrons, respectively, m_e is the mass of the electron, $\epsilon_{\gamma\delta\lambda\mu}$ is the Levi-Civita tensor, S is the polarization vector of the incident electron, P the four-momentum of the target, and k (k') the four-momentum of the incident (scattered) electron. The expression $\epsilon_{\gamma\delta\lambda\mu} S^{\gamma} P^{\delta} k^{\lambda} k'^{\mu}$ is strictly zero for beam with $\vec{S}$ along $\vec{k} \times \vec{k}'$ and no BNSSA will occur, unless, a non-zero imaginary amplitude is present, which requires multi-photon exchanges [13]. Stated more explicitly,

$$A_{\rm n} \propto 2 Im T_{2\gamma} T^{*}_{1\gamma}, \quad (2)$$

where $T_{1\gamma(2\gamma)}$ is the one (two) photon exchange amplitude. BNSSA measurements can play an important role in our understanding of the TPE process because of their direct access to the imaginary part of the TPE amplitude.

As a potential background to high precision Parity Violation Electron Scattering (PVES) measurements, A_n were measured in experiments such as Qweak [14] for elastic scattering and the 6 GeV PVDIS experiment [15, 16] for DIS. However, the precision goal of these A_n measurements was set by A_n contimination in the main PVES asymmetry observable, and typically only a day of beam was dedicated to such measurement each time. One reason that a high precision, dedicated measurement of the BNSSA in DIS has not yet been performed is because of the use of small-acceptance spectrometers. Combined with the very small size ($\approx$ ppm) expected for the asymmetry, it requires significant beam time to reach a meaningful precision for asymmetries in DIS. A key feature of the proposed measurement is that the large acceptance of the Solid Large Intensity Device (SoLID) allows a high precision measurement of BNSSA in DIS within a reasonable amount of beam time.

1.3 Existing SSNA Measurements

1.3.1 Early BNSSA Measurements at SLAC

Interests in two-photon exchange originated as early as the first DIS experiment(s) at the Stanford Linear Accelerator Center (SLAC). In a very early experiment [17], the ratio of e^+p and e^-p elastic-scattering cross sections was measured at Q^2 values between 0.20 and 5.00 (GeV/c)^2. The measured ratio, after radiative corrections, are consistent with unity, with uncertainty ranging from ±0.016 to ±0.123. These results gave the first limit for the size of TPE effects, but have rather large uncertainties in the modern standard.

1.3.2 BNSSA Elastic Measurements

Measurements of BNSSA in elastic scattering were routinely conducted in PVES experiments as part of the systematic effect study. With the realization that TPE may have a non-negligible effect in elastic form factor measurements, a number of experimental programs have measured the BNSSA in elastic scattering for a number of nuclei over a variety of different kinematics. These investigations have thus far shed some light onto kinematic and nuclear mass dependence of the effect. Figure 2 is a compilation of the current BNSSA measurements for elastic scattering taken at different experimental facilities, including data taken at both forward and backward angles. In general, comparison between theory predictions and experimental data show a reasonable agreement. However, a recent measurement at MAMI [18] shows a disagreement with available predictions. These disagreements have been surmised to be due to missing intermediate states in theory calculations and point to the need for further experimental and theoretical investigation to better understand these discrepancies.

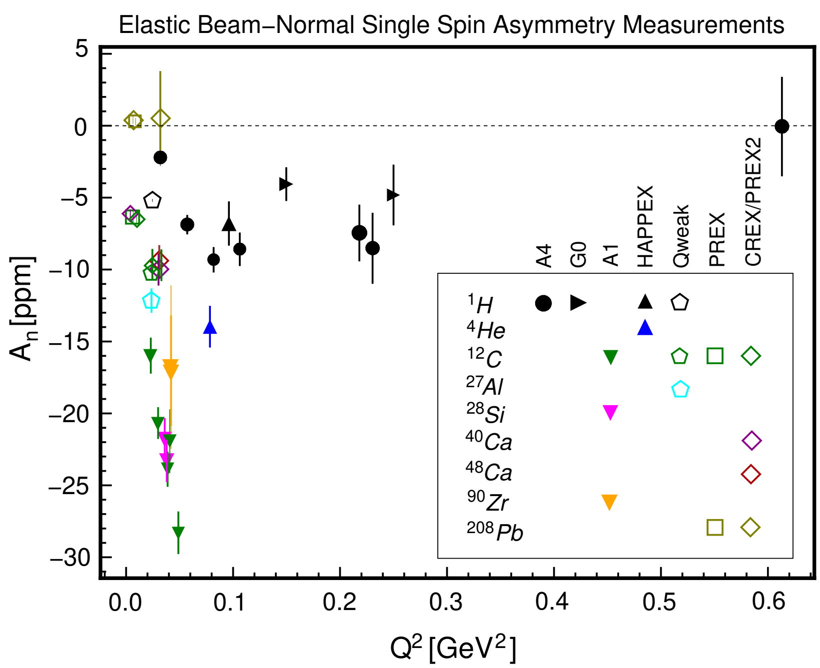

Figure 2: Compilation of existing elastic BNSSA measurements. Data from [18, 19, 20, 21, 22, 23, 24]

1.3.3 BNSSA DIS Measurements

At present, no robust, high-precision study of the BNSSA in DIS has been made. The only existing data with ppm-level uncertainty are measurements made to estimate background in the JLab 6 GeV PVDIS experiment [16], see Fig. 3. The uncertainty is large, and further exploration in the DIS region with high precision is clearly desired. As suggested by Afanasev: "If we can measure this to ±5 ppm, it will be very useful information. Even ±10 ppm is a big step, because pretty much nothing is known for this in DIS" [25].

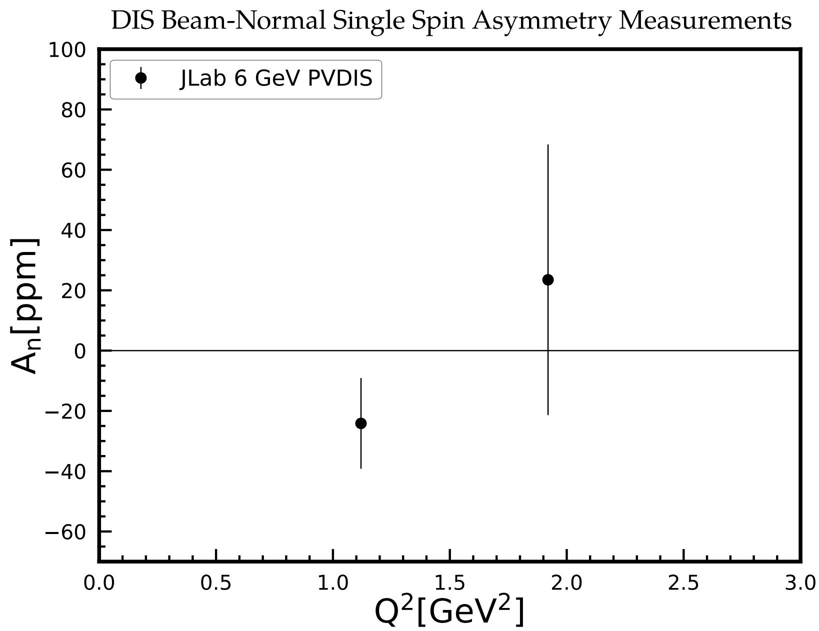

Figure 3: The DIS BNSSA for the deuteron, data from the JLab 6 GeV PVDIS experiment [16].

1.3.4 TNSSA Measurements

Similar to BNSSA, TNSSA also provides insight into TPE processes. Because the size of the asymmetry, depicted in Eq. (1), is proportional to the mass of the polarized particle of interest, TNSSA is expected to be much larger than BNSSA, making it relatively easy to measure. To study TNSSA, often denoted A_y, the target is polarized normal to the electron scattering plane with its spin direction flipped periodically, and the cross section asymmetry is formed between the two target spin directions. TNSSA was measured by several experiments. Most notably, TNSSA was measured at JLab using a polarized ^{3}He target, used effectively as a polarized neutron target, for both DIS [26] and quasi-elastic scattering [27]. Figure 4 shows these neutron results and a clear evidence of non-zero TNSSA that is beyond the single parton-model prediction (see next section for details). On the other hand, similar experiments carried out at HERMES on a polarized hydrogen target [28] showed that the proton TNSSA is consistent with zero (within a 10^{-3} level uncertainty) in the region $0.007 < x < 0.9$ and two Q^2 ranges of 0.25 GeV^2 $< Q^2 < 1$ GeV^2 and $1 < Q^2 < 20$ GeV^2, and for both electron and positron beams. Clearly, further investigation in the TNSSA is desired and there is a plan to extend the measurement on both polarized proton and polarized ^{3}He as part of the approved SoLID SIDIS program [29].

1.4 Theoretical Predictions for SSNA

At the present, the number of theoretical predictions for BNSSA in the DIS regime is limited. Parton model predictions exist with the assumption that the interactions occurs with a single quark, such that both photons of the TPE couple to a single quark in the target nucleon. Based on prior derivation for two point-like fermions[30], Metz et.al [12] have expressed the BNSSA for DIS as:

$$A_{TU} = \alpha \frac{m_e}{2Q} |S_T| \sin(\phi) \frac{y\sqrt{1-y}\sum_q {e^3}_q q(x)}{[1+(1-y)^2]\sum_q {e^2}_q q(x)}, \tag{3}$$

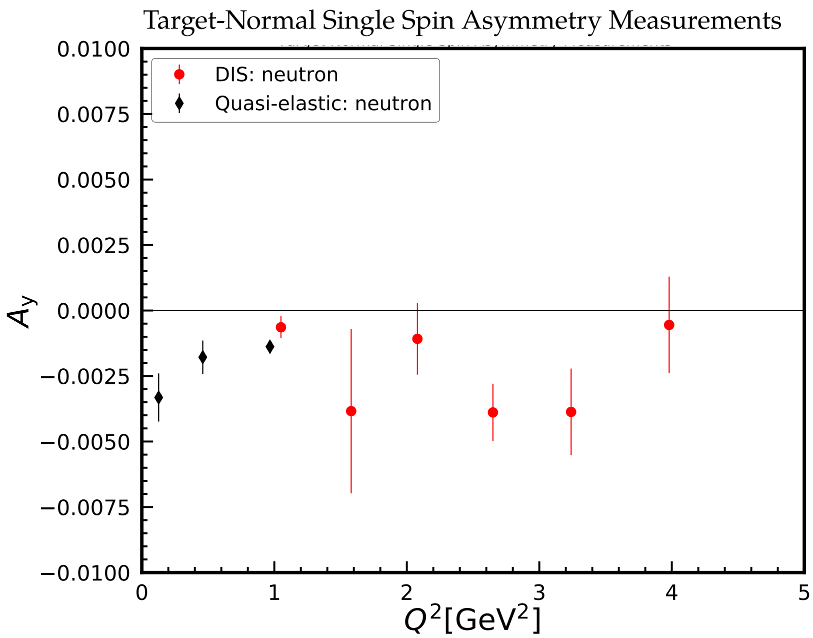

Figure 4: Target Normal Single Spin Asymmetry of the Neutron measured by JLab E07-013 [26] and E05-015 [27]

where α is the fine-structure constant, m_e is the electron mass, S_T is the polarziation of the electron, y is the fractional energy transfer, and $q(x)$ are the parton distribution functions (PDFs) with the relevant quark charge denoted as e_q. Similarly, Gorchtein et.al [31] calculated the BNSSA in elastic scattering at very high Q^2, and provide an expression for BNSSA of an elementary fermion, from which one can make an approximation to estimate the asymmetry in DIS. Both of these models give predictions which estimate a BNSSA in the DIS region to be in the range between 0.6 - 6 ppm. Enhancements to the BNSSA due to higher order effects, beyond those included in the parton model calculations, would result in larger measured BNSSAs values [32]. While existing DIS data [16] (see section 1.3.3) showed a hint that BNSSA may be at 10 ppm level, they have large uncertainties and higher precision measurements are needed to establish non-zero, ppm-level values of BNSSA in DIS.

The situation for TNSSA is different. Parton model calculation for the neutron, in which both photons couple to a single quark, predicted an $A_y^n \approx 10^{-4}$ [33]. On the other hand, considerations in which the electron exchanges two photons with different quarks predict an enhancement of A_y^n to the level of 10^{-2} [34], in good agreement with the JLab TNSSA data shown in Fig. 4.

Dedicated measurements focusing on TNSSA such as those planned as a run group experiment with the SoLID SIDIS program [29], and those focusing on BNSSA such as the one proposed here, would provide an important step in the understanding existing data, in constraining TPE models, and in studying the validity of parton model in a variety of kinematic regimes.

2 Experimental Setup

2.1 Overview

We propose to measure the beam-normal single spin asymmetry in inclusive deep inelastic scattering using a 40 cm liquid hydrogen target. We will measure the BNSSA using a 6.6 and 11 GeV electron beam polarized in the horizontal direction and the beam spin is flipped between pointing beam-left and beam-right following the helicity sequence $(+--+$ or $-++-)$. A luminosity on the order of 7.5×10^{38} $\text{cm}^{-2}\text{s}^{-1}$ is expected for a 40 cm liquid hydrogen target and a 70μA beam current. The scattered electrons will be detected using the PVDIS configuration of the SoLID detector. The PVDIS configuration of SoLID with its baffle system has been designed and studied extensively for the approved E12-10-007 experiment – "Precision Measurement of Parity-violation in Deep Inelastic Scattering Over a Broad Kinematic Range" or simply referred to as "SoLID PVDIS" or "PVDIS" [35] – and is particularly suitable for the proposed measurement.

Defining the electron beam direction to be $\hat{z}$ and the unit vector $\hat{y}$ pointing vertically up, and assuming that the beam spin is polarized in the horizontal $(\hat{x})$ direction, the experimentally extracted BNSSA can be expressed as:

$$A_{\perp} = \frac{1}{P_b} \cdot \frac{N^{\uparrow}(\phi) - N{\downarrow}(\phi)}{N{\uparrow}(\phi) + N{\downarrow}(\phi)} = A_n \sin(\phi) \;, \tag{4}$$

where P_b is the beam polarization, $N^{\uparrow}$ and $N^{\downarrow}$ refer to the charge normalized event counts detected for the incoming electron spin pointing in the $+\hat{x}$ (beam-left) and $-\hat{x}$ (beam-right) directions, respectively, and ϕ is the azimuthal angle. By flipping the spin of the beam (spin left $\leftrightarrow$ right), we can measure A_n by analyzing the ϕ dependence of the measured asymmetries. The transverse beam polarization of the electron beam is expected to be $P_b \approx 85\%$ for the proposed experiment.

2.2 Cryogenic Target System

The proposed experiment will use a 40-cm liquid hydrogen target, the same which is designed for the PVDIS experiment [35]. Along with the cyrogenic target, a dummy target mimicking the cryo-target endcaps and additional solid targets will be included in the target system for calibration purposes.

While the PVDIS experiment is expected to use a 50 μA beam current, we expect that a 70 μA beam current should pose no problem on the accelerator capacity [36] nor target cooling power. A 70 μA beam on a 40-cm liquid hydrogen target will require 1.4 kW of cooling power, more modest than the 2.5 kW of the Qweak target which was employed at JLab from 2010 to 2012. In addition, the MOLLER experiment will require a 5 kW ESR2, far exceeding the need of the proposed measurement.

The liquid hydrogen and deuterium may become slightly polarized in the magnetic field of the solenoid. This would result in an asymmetry unrelated to the physics of interest. In the case of (ortho-)hydrogen, a 1.5 T field and 20 K temperature would result in a polarization of less than 10^{-4} along the direction of the field (longitudinal for SoLID). The use of pure para-hydrogen would reduce this effect because para-hydrogen would not be polarized under high fields. At room temperature, hydrogen is 25% para and 75% ortho. As temperature decreases, most ortho would transition to para hydrogen, reaching a 99% pure para state within a week without the use of a catalyst [37]. In the aid of a catalyst (such as the iron piping existing in the cryotarget system), the ortho$\rightarrow$para transition will be completed within a day [38]. We discuss quantitatively the effect of target polarization on the measurement in Section 3.2.2.

Localized heating of the target from the electron beam can result in density fluctuation of the cyrogenic target, commonly referred to as target boiling. This effect can cause a reduction in the density of the target as well as noise in the asymmetry that mimics the statistical uncertainty. To minimize effects related to localized heating of the the target, the electron beam will be rastered to 4×4 mm^2 with a square pattern. We note that specially designed cryogenic targets have been utilized for high-precision PVES experiments at JLab, including Qweak. In addition, we expect a dedicated target study to be carried out for the approved PVDIS experiment. We thus do not expect target heating to be a significant contribution to the uncertainty of the proposed measurement.

The total thickness of the aluminum endcaps of the cryotarget cell will be approximately 270 μm (120 μm upstream, 150 μm downstream). In order to account for possible background and dilution from $e-^{27}$Al scattering, dedicated runs with an aluminum dummy target will be used to determine the yield of the background. We take into account target endcap effect in our systematic study, see Section 3.2.3.

2.3 The SoLID Spectrometer in its PVDIS Configuration

The proposed experiment will use the SoLID spectrometer [39], for which there are currently 5 approved experiments – on SIDIS, PVDIS, and J/Ψ production – along with an additional 6 run group experiments, including measurement of TNSSA alongside SIDIS [29]. The SoLID spectrometer is a large acceptance device which is capable of operating under a high radiation environment and can handle high background and high rates. SoLID has two configurations: PVDIS and SIDIS, allowing it to meet the broad experimental requirements of the SoLID program. The proposed experiment plans to utilize SoLID in its PVDIS configuration, see Fig. 5. To handle the up to 10^{39} cm$^{-2}s^{-1}$ luminosity, a baffle system is designed to greatly reduce the total background – in particular charge-neutral and low-energy charged background – in the detectors while reducing the acceptance of DIS electrons by about a factor 3. The detector system of SoLID in the PVDIS configuration consists of GEM trackers, light gas Cherenkov, and electromagnetic calorimeter, which we describe in the next section in more detail.

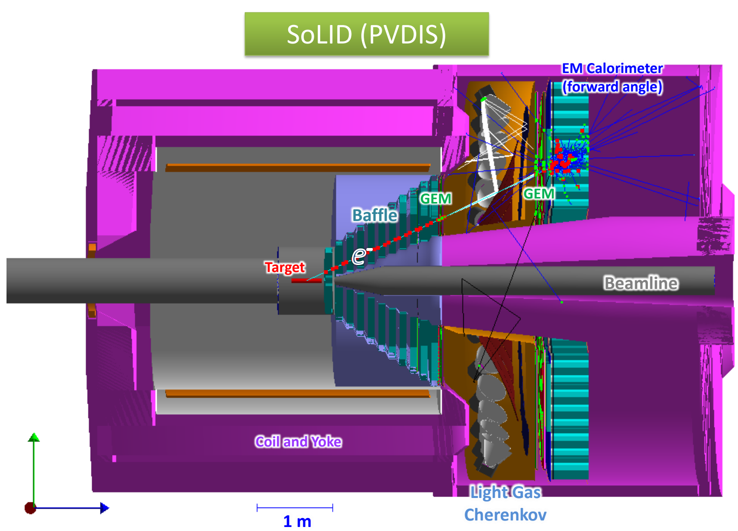

Figure 5: Side view of the SoLID apparatus in the PVDIS configuration. For details see [39].

2.4 Detector System

2.4.1 GEM

Particle tracking for SoLID will be performed by Gas Electron Multiplier (GEM) trackers. The GEM trackers are ideal for the SoLID detector due to the need for high resolution tracking coupled with the high-rate environment over a large area. More specifically, we expect the GEMs to provide a position resolution of 70 μm with rates over 100 MHz per cm^2 [39]. For the PVDIS configuration, five layers of GEMs will be used, three before the light-gas Cherenkov and two after, see Table 1. Each layer will consist of 30 sectors in the azimuthal direction, matching the baffle design. This layout will allow for a 1 mrad polar angle and a 2% momentum resolutions.

Layer	Z (cm)	R$_{min}$ (cm)	R$_{max}$ (cm)	Surface area (m^2)
1	157.5	51	118	3.6
2	185.5	62	136	4.6
3	190	65	140	4.8
4	306	111	221	11.5
5	315	115	228	12.2

Table 1: Location of the five GEM layers in the SoLID PVDIS configuration. The coordinate Z refers to the position along the beamline with target centered at $z = 0$, while $R_{\min,max}$ refer to the inner and outer radii of each layer.

2.4.2 Light Gas Cherenkov

A main component of the particle identification (PID) in the PVDIS configuration is the light gas Cherenkov (LGC) detector. The LGC is comprised of an approximate 105 cm long radiator (z), with an inner (outer) diameter of 71 (85) cm and is divided into the 30 sectors, each consisting of a pair of mirrors and one PMT onto which light is reflected [39]. The tank will be filled with either CO_2 or N_2 gas. With the above design features, the LGC is expected to have a nominal pion rejection on the order of 10^3 while maintaining an electron efficiency close to 95%.

2.4.3 Segmented Electromagnetic Calorimeter

The segmented electromagnetic calorimeter (ECal) consists of a preshower and a shower section. The preshower configuration is that of a $2X_0$ pre-radiator and a 2-cm thick scintillator. The shower is a Shashlyk type sampling caloriemter with alternating layers of scintillator and lead absorber with wave-length shifting fibers interleaved through the layers. The scintillation light is absorbed and re-admitted by these wavelength shifting fibers and eventually captured by PMTs. The segmentation of the calorimeter, at 100 cm^2 in transverse size, was designed to best satisfy the requirements of the SoLID physics program, which includes the necessity of covering a large area as well as operating in a high radiation environment. The specific characteristics of the calorimeter are provided in Table 2.

	Performance
π^- rejection	[50:1]
e$^-$ efficiency	90%
Energy resolution	$\delta E/E \leq$10%/$\sqrt{E}$
Position resolution	$\leq$ 1 cm
Radiation hardness	$>\sim$400 kRad

Table 2: Basic characteristics of the SoLID EM Calorimeter.

2.4.4 Trigger and Data Acquisition System

The proposed measurement will utilize the same trigger and DAQ system as the SoLID PVDIS experiment. To keep the trigger rate at a manageable level, the detector electronics are divided into 30 sectors, each with a separate trigger. For each sector, the trigger will be a coincidence between the LGC and the ECal with a 30 ns coincidence window. The current estimate of the DAQ limit is 10 kHz per sector or 300 kHz total. This DAQ limit is the primary reason that we plan to use a 70μA current at 6.6 GeV.

2.5 Transversely Polarized Beam

The electron beam at CEBAF is produced via photo-emmission from circularly polarized laser incident upon a GaAs photocathode [40]. The initial polarization of the beam is longitudinal and then the orientation is manipulated by two Wien filters and a set of solenoids. The first Wien filter rotates the spin to vertical and then the solenoid rotates the polarization to the horizontal plane and perpendicular to the beam line (so called "flip-left" or "flip-right" setting). The second Wien filter rotates the polarization about the vertical axis to the desired launch angle from the injector.

As the electron beam is bent around the racetrack-shaped accelerator of CEBAF and into the individual experimental halls, the direction of the horizontal polarization rotates due to spin precession. Since the bending angle into the individual halls differ, the launch angle can only be optimized for one hall. However, by adjusting the total beam energy and the energy imbalance between the North and South linacs, near maximum longitudinal or transverse (horizontal) polarization can be delivered to all halls at certain energies [36, 41].

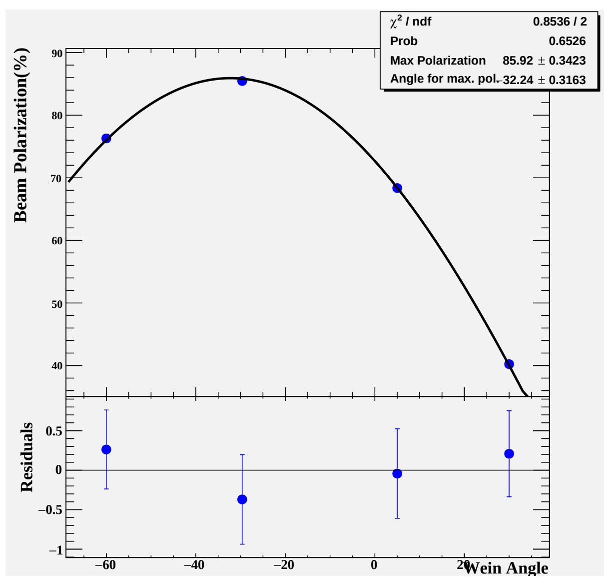

Figure 6: Spin dance performed in Hall C in February 2019

For the proposed measurement, it is desired that the beam is fully polarized in the transverse direction. In the case that the Wien filter setting is slightly off the ideal value, there will be a small longitudinal polarization of the beam into the hall. We denote this as S_L. This component can be measured using a procedure called spin-dance, see Fig. 6. Comparison of spin-dance with other beam diagnostic methods shows that the Wien filter setting can be determined comfortably to a level of $3°$ (5% of the maximum polarization) in precision, though $1°$ has been reached with careful study [42]. On the other hand, given that S_L would induce background from PVDIS asymmetry which is large, we consider a simultaneous fit of A_n and S_L from the measured asymmetry in addition to the method of subtracting the expected S_L background from the measurement, see Section 3.2.6.

2.6 Beam Polarimetry

Beam polarization measurements are to be made with the Hall A Moller polarimeter which requires a longitudinally polarized beam. Therefore the horizontal Wien filter at the injector will have to be adjusted to change the launch angle by +/- 90 degrees prior to each Moller measurement. This process will have to be coordinated with the other halls since it will change the beam polarization they receive for the length of the Moller measurement (8-16 calendar hours). Given that other upcoming PVES experiments in Hall A requires 0.4-0.5% precision polarimetry, we expect to reach the same precision for longitudinally polarized beam. Additional uncertainty could come from rotation of the Wien filter, though this adds only a negligible 10^{-3} uncertainty to the polarimetry measurement.

In summary, the proposed experiment does not require any new or additional equipment for the beam polarization measurement, beyond what has already been proposed by the SoLID or other (MOLLER) collaborations. The Mott polarimeter in the injector can be used without changing the Wien filter angle, to provide a $2-3\%$ precision on the beam polarization, and can be used in addition to Moller polarimetry.

3 Rates, Uncertainties and Projected Results

3.1 Kinematics Settings and Rate Estimation

A simulation based on the SoLID detector was used to make reliable estimates about the feasibility and overall impact of the experiment. The simulation is GEANT4 based, using the GEMC framework to implement each of the detector geometries. The general PVDIS setup was used when making the estimates. Estimates were made using a 40 cm liquid hydrogen target along with the full detector setup and the inclusion of baffles. All estimates were made assuming a total of 30 production days of running, split between 6.6 and 11 GeV (17 and 13 days), along with an 85% beam polarization. Figure 7 illustrates the kinematic coverage in x and Q^2 with the expected rates for such running conditions. Given the experimental conditions outlined, an estimate of the statistical uncertainty is shown in Fig. 8.

3.2 Systematic Uncertainties

The proposed experiment will be the first dedicated measurement of the beam-normal single spin asymmetry in deep inelastic scattering. The total uncertainty of the extracted BNSSAs will largely be statistics dominated. Many of the systematic uncertainties will enter at a level not expected to play a dominate role. The main systematic uncertainty for the experiment is from the longitudinal component of the electron beam polarization during the nominal transverse polarization running. We will discuss it and briefly discuss several other sources of systematic uncertainties and their contributions to the measured asymmetry.

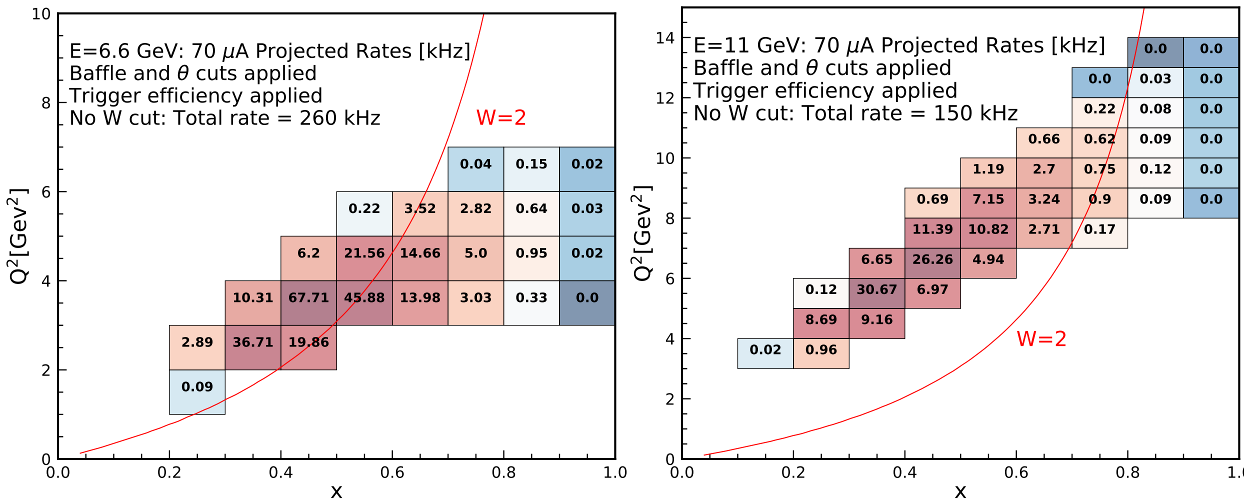

Figure 7: The expected rate in the SoLID PVDIS configuration for the 6.6 GeV (left) and 11 GeV (right) settings. The rates in kHz are shown for each (x, Q^2) bin. A DIS cut of $W > 2$ GeV has been applied.

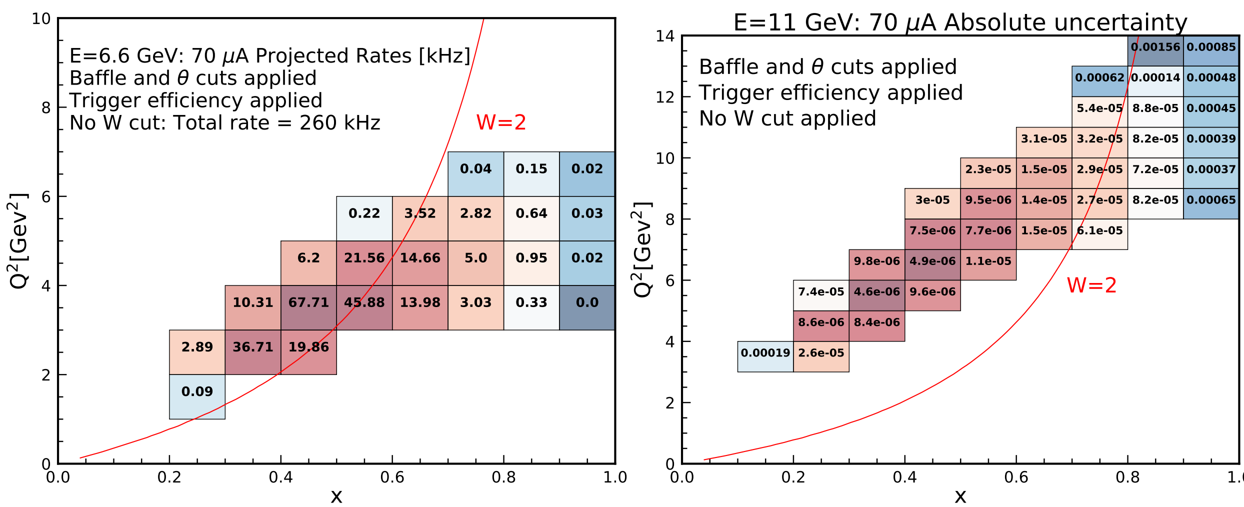

Figure 8: The expected absolute uncertanties in the SoLID PVDIS configuration for the 6.6 GeV (left) and 11 GeV (right) settings.

3.2.1 Beam Polarimetry

While upcoming PVES experiments aim to achieve sub-1% on beam polarimetry, we anticipate that a 1% overall uncertainty due to beam polarization to be both (comfortably) achievable and precise enough for the proposed measurement.

3.2.2 Target polarization

The ortho hydrogen under 20 K and 1.5 T would be polarized to 7×10^{-5}. The para hydrogen would not have any polarization. As described in Section 2.2, it is relatively straightforward to obtain $> 99\%$ pure para hydrogen at 20 K. This already limits the possible contribution from target polarization to the measured asymmetry to below 0.5 ppm. The actual physics asymmetry of a transversely polarized beam incident on a longitudinally polarized proton will further reduce this effect. We expect the effect from the polarization of the target material to be under 0.1 ppm.

3.2.3 Target endcaps

As described in Section 2.2, the 40-cm long liquid hydrogen target has two aluminum endcaps of thickness 120 μm and 150 μm for the entrance (upstream) and exit (downstream) portions, respectively. The yield of the $e-^{27}$Al scattering will be determined using an aluminum dummy target. On the other hand, the statistics from such dummy target runs will not be sufficient to determine A_n on aluminum to high precision. Since no robust calculation for A_n is available for ^{27}Al, we will not apply a correction to the measured hydrogen asymmetry. Instead, we assume that A_n for ^{27}Al DIS to be no more than factor 2 different from A_n for hydrogen, which will result in a 5% relative uncertainty.

3.2.4 Q^2 Determination

The PVDIS experiment has a requirement of $\approx 0.2\%$ uncertainty in the determination of Q^2. This has required an intensive study of the experimental design to understand and show how to meet this requirement, see [35]. We assume the same can be achieved for the proposed measurement. We also note that while it is expected that A_n may depend on Q^2, our goal is to determine if A_n is significantly larger than the simple parton-model prediction and the 0.2% precision of the Q^2 more than sufficient in this context. Therefore, we do not anticipate Q^2 determination being a major systematic uncertainty.

3.2.5 Particle Background

A major background for DIS experiments comes from charged pions. Detailed estimates for pion contamination have been made for the PVDIS experiment, and are applicable for the proposed measurement. Utilizing the LGC and the ECal, a pion suppression factor of 2×10^5 is expected for off-line data analysis and the contamination is estimated to be at 1% level or less for momentum above 2 GeV/c.

Another significant background for DIS are electrons from pair production processes. In Fig. 9 we show an estimate (in percentage) of the anticipated background due to pair production. The estimates were produced using the common Wiser's fit, bench-marked with Hall C 12 GeV data [43]. We plan to reverse the SoLID magnet polarity to measure the yield of this background and treat it as a dilution effect to the measured asymmetry. The uncertainty due to pair production background should be below 0.1% for majority of the kinematic bins.

3.2.6 Beam Longitudinal Spin

In the case that the beam carries a longitudinal polarization, it will add a parity-violating (PVDIS) asymmetry to the measured data. The PVDIS asymmetry on the proton is independent of ϕ but is generally proportional to Q^2:

$$A_{\mathrm{PVDIS},p} = \frac{3G_F Q^2}{2\sqrt{2}\pi\alpha} \frac{\left[(2U^+ g_{AV}^{eu} - D^+ g_{AV}^{ed}) + Y(2u_V g_{VA}^{eu} - d_V g_{VA}^{ed})\right]}{(4U^+ + D^+)}, \quad (5)$$

where we have abbreviated PDFs $q^+ \equiv q(x,Q^2) + \bar{q}(x,Q^2)$ and $q_V \equiv q(x,Q^2) - \bar{q}(x,Q^2)$ ($q = u,d,c,s$) and furthermore $U^+ \equiv u^+ + c^+$ and $D^+ \equiv d^+ + s^+$, and have assumed $c = \bar{c}$ and $s = \bar{s}$

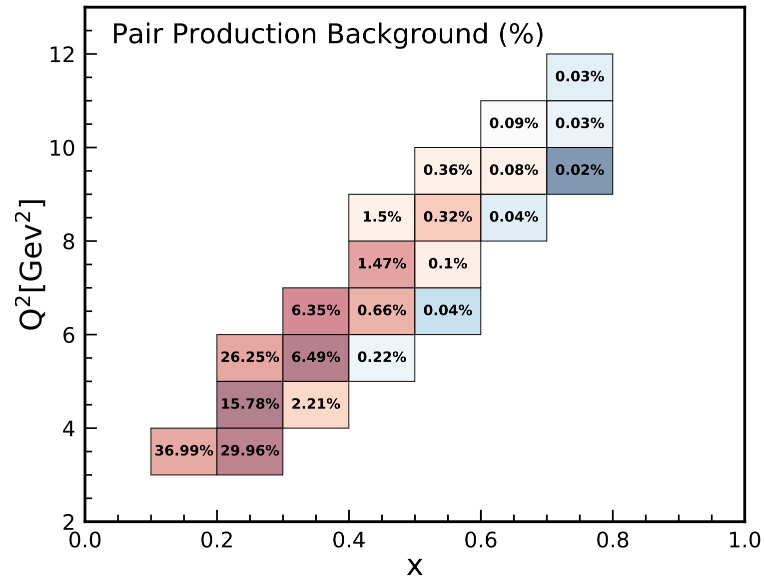

Figure 9: Estimate of the pair produced background using Wiser fit for the 11 GeV setting. A reduced kinematic region was used to make the estimate. The largest background occurs at low x and high y values.

(and thus $c_V = s_V = 0$). The function Y is defined as $Y = [1-(1-y)^2]/[1+(1-y)^2]$. The $g^{eq}_{AV,VA}$ are electron-quark effective neutral-current couplings and are well defined in the Standard Model, and G_F is the Fermi constant. One can thus calculate the x and Q^2 dependence of the PVDIS asymmetry background using SoLID simulation, and the measured asymmetry will consist of two contributions: the BNSSA that is $\phi-$dependent, and an additional term $S_L A_{\mathrm{PVDIS},p}(x, Q^2)$ that is independent of ϕ where S_L is the beam longitudinal spin component. The value of S_L can also be measured through a spin-dance procedure and determined to a 3° level, as described in Section 2.5. However, due to the large size of PVDIS asymmetry, at about 70-80 ppm multiplied by Q^2 values (in GeV^2), we found it is advantageous to treat S_L as a fitting parameter rather than using spin-dance result, see Section 3.3.

3.2.7 Beam In-Plane Transverse Polarization

If the spin of the incoming electron is polarized transversely but in the scattering plane, there can be a parity violation asymmetry for scattering off an unpolarized target. It would be similar to the asymmetry of an unpolarized electron scattering off a polarized proton with opposite spin direction, except that one swaps out the proton polarized structure functions $g^{\gamma Z}_{1,2,3,4,5}$ by the counterparts of a Dirac fermion (the electron). Experimentally, such asymmetry will show up as a $\cos(\phi)$ contribution. We expect this asymmetry to be that of typical PVES and further suppressed by m_e^2/Q^2 because of the transverse spin, and is much below the ppm level. In any case, it can be calculated precisely using a complete leptonic tensor that accounts for transverse spin of the electron, and the typical DIS hadronic tensor that can be readily expressed in terms of PDFs.

3.2.8 Summary of Systematic Uncertainties

We show in Table 3 a summary of all systematic uncertainties. As described in the next section, we expect that statistical uncertainty on the extracted A_n to be at 10% (2 ppm) level or larger and dominate the uncertainty of the proposed measurement. At the mean time, the effect of beam longitudinal polarization and spin angle are dealt with in the data analysis step and are not shown in the table.

Target endcaps	5%
Polarimetry	1.0%
Particle background	1.0%
Q^2 determination	0.2%
Target polarization	under 0.1 ppm
Total systematic	5.2%

Table 3: Systematic uncertainty for the proposed measurement, shown as relative uncertainty in the measured asymmetry unless specified otherwise.

3.3 Data Analysis and Projected Results

The raw BNSSA asymmetry will be determined according to:

$$A_{\text{raw}} = \frac{1}{P_b}\frac{N^{\uparrow}(\phi) - N^{\downarrow}(\phi)}{N^{\uparrow}(\phi) + N^{\downarrow}(\phi)}; \tag{6}$$

where P_b is the beam polarization, and $N^{\uparrow}$ and $N^{\downarrow}$ are charge normalized yields for electrons polarized perpendicular – left and right or up and down – to the electron's momentum, respectively. The BNSSA, A_{n}, can subsequently be extracted from the raw asymmetry distributions.

As mentioned in the previous section, a longitudinal component of the beam polarization (S_L) will result in a residual PVDIS asymmetry. This can introduce a sizable uncertainty in the measured asymmetry and the subsequently extracted BNNSA. To understand the effect the S_L will have on our projected BNSSA, we performed a multi-parameter fitting study as follows:

1. Perform a simulation using the GEMC SoLID Monte Carlo generator to determine the statistical precision that can be achieved in each (x, Q^2) bin given the luminosity, acceptance profile, and DAQ rate limit of the PVDIS configuration. The beam polarization P_b is corrected in this step, i.e. $\Delta A^i_{\text{stat}} = 1/\sqrt{N_i}/P_b$ with N_i the event count expected for the i^{th} bin.

2. Generate pseudo-data on the asymmetry following a $A_{\text{n}}\sin(\phi)$ form in each Q^2 bin, with a random number r_i generated in each Q^2 bin to mimic the effect of the statistical fluctuation based on the uncertainty calculated from the previous step. The value of A_n is assumed to be a constant 20 ppm.

3. Generate a random number r_s within 5% of the maximum polarization, to account for the longitudinal component S_L of the beam polarization. This random number applies to all Q^2 bins of the same beam energy. The pseudo data in each Q^2 bin now read:

$$A^{i^{th}\text{bin}}_{\text{raw,pseudo-data}} = 20\text{ ppm}\sin(\phi) + r_i\Delta A^i_{\text{stat}} + r_s A^i_{p,\text{PVDIS}}$$

   where $A^i_{p,\text{PVDIS}}$ is the proton PVDIS asymmetry calculated for the i^{th} bin.

4. From here, there are 3 possible analysis methods to extract A_n:

- Subtract $S_L A_{\rm PVDIS}$ from the pseudo data and then fit the $\sin\phi$ form. In this case, the value of S_L is the same as r_s but the 3° (5%) uncertainty in S_L needs to be accounted for in the asymmetry after the subtraction.
- Perform a multi-parameter fit of the form $A_{\rm n}\sin(\phi) + BA_{\rm PVDIS}$, where D is a parameter that corresponds the longitudinal component, $S_{\rm L}$.
- Perform a $\sin\phi$ weighted integral in ϕ to extract A_n. The S_L component vanishes with the integration.

We studied all three methods described above in order to best minimize the total uncertainty on the extracted A_n. We found that the multi-parameter fit produces the best result. The multi-parameter fit takes the general form, for each bin:

$$
\begin{aligned}
f_1 &= C_1 \cdot \sin(\phi + \phi_{\rm off}) + D \cdot A_{p,\rm PVDIS} \\
f_2 &= C_2 \cdot \sin(\phi + \phi_{\rm off}) + D \cdot A_{p,\rm PVDIS} \\
&\vdots \\
f_N &= C_N \cdot \sin(\phi + \phi_{\rm off}) + D \cdot A_{p,\rm PVDIS},
\end{aligned}
\tag{7}
$$

where f_i is the fitting function for the pseudo data in the i^{th} bin, the C_i coefficients correspond to the fitted BNSSA in each Q^2 bin, $\phi_{\rm off}$ is a phase factor that accounts for possible mis-alighment of the detector, and D is a parameter that corresponds to the longitudinal component of the beam polarization S_L. We found the fitted uncertainty on S_L to be at 1% level or below, better than the 3° (even the 1°) uncertainty of the Wien angle determination.

3.4 Projected DIS Results

Applying the methods outlined above, we were able to make reasonable estimates of the BNSSA extraction and its uncertainties. In Figs. 10 and 11, we show the ϕ dependence of A_n across different Q^2 for 6.6 and 11 GeV, respectively. Both statistical and systematic uncertainties are included along with a DIS cut of $W > 2$ GeV.

By performing the multi-parameter fit of Eq. (7), we extracted the individual BNSSA values for each Q^2 bin of size 1 GeV^2. These are shown in Fig. 12 and 13 for the 6.6 and 11 GeV settings, respectively. Additionally, the individual BNSSA values from different Q^2 bins were combined, which provided an uncertainty of 2.1 and 3.8 ppm. A summary plot of the extracted BNSSA values is given in Fig. 14 and compared with the existing 6 GeV PVDIS data. The systematic uncertainty (not shown) is expected to be $\approx 5\%$ and is much smaller than the statistical uncertainties.

Finally, we note that inelastic events in the nucleon resonance region will be accepted by SoLID detectors and we can in principle extract A_n in the nucleon resonance region. However, our knowledge on the resonance $A_{\rm PV}$ is limited, and one cannot perform a precise determination of resonance A_n without studying carefully the precision on $A_{\rm PV}$ as well. Therefore, we will present the fitted results on the resonance A_n in Appendix A, accounting only the statistical uncertainty.

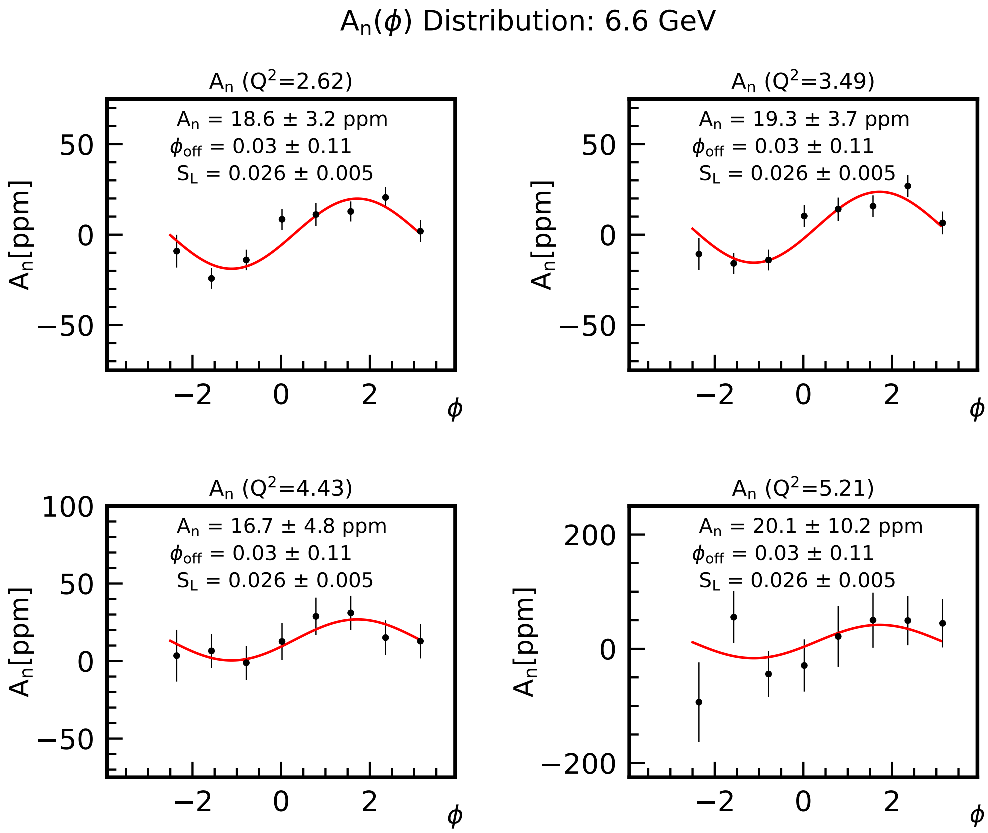

Figure 10: Generated pseudo data for the 6.6 GeV beam energy setting with a $W > 2$ GeV cut to select DIS events. A common value of the 20 ppm was assumed for the size of A_n. An input value of 0.0150 was used an input for S_L. The uncertainty in the fitted S_L coefficient was found to be at a level of 0.52%.

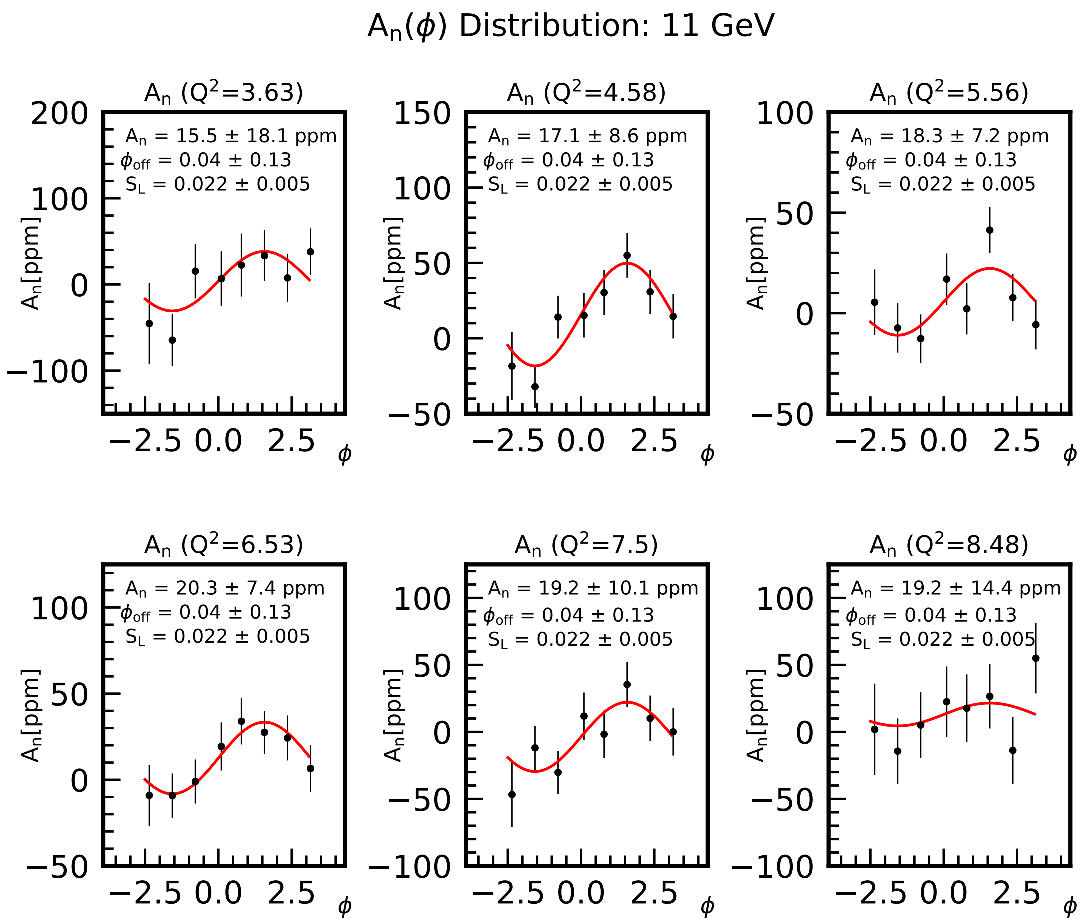

Figure 11: Same as Fig. 10 but for the 11 GeV beam energy setting. The uncertainty in the fitted S_L coefficient was found to be at a level of 0.47%.

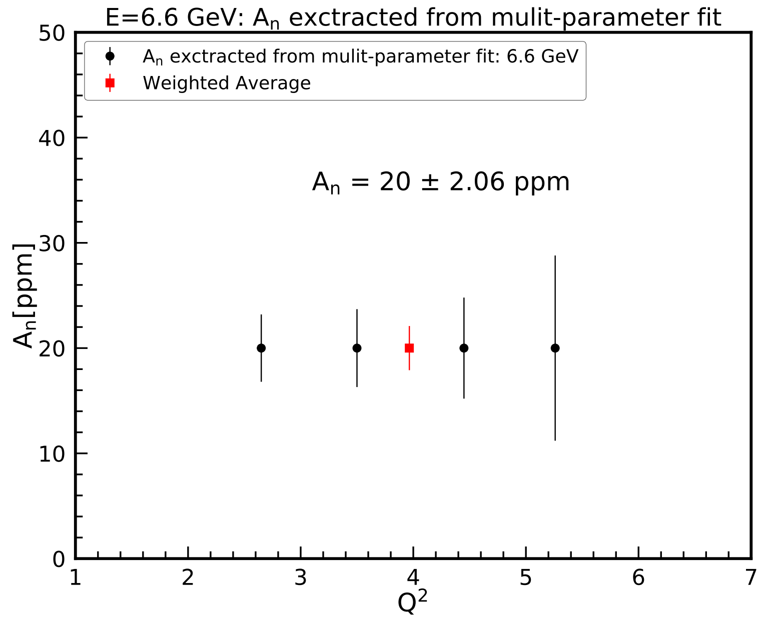

Figure 12: Projected results on DIS BNSSAs extracted with a multi-parameter fit for the 6.6 GeV data. The black dots represent the fitted BNSSA in each Q^2 bin while the red square at the center is the weighted average combined over all Q^2 values. The projections were made assuming 17 PAC days of running at 70μA.

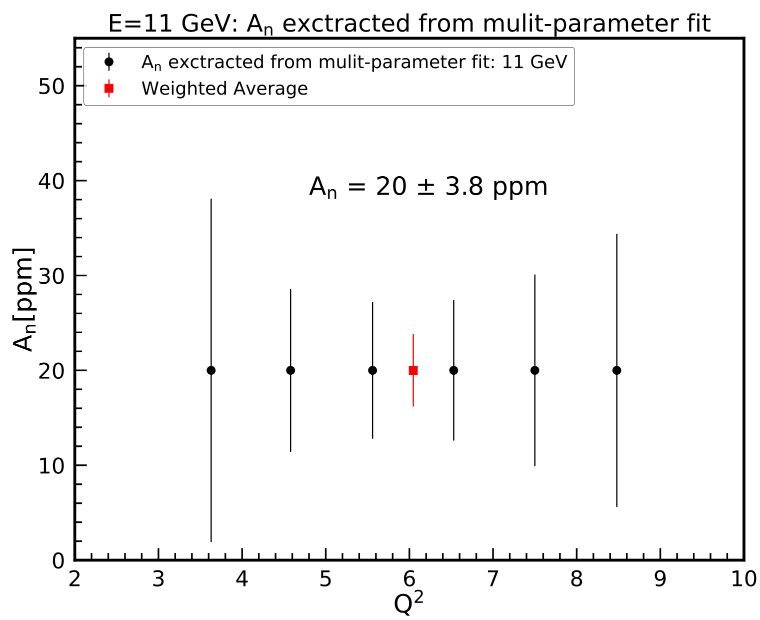

Figure 13: Projected results on DIS BNSSAs extracted with a multi-parameter fit for the 11 GeV data. The black dots represent the fitted BNSSA in each Q^2 bin while the red square at the center is the weighted average combined over all Q^2 values. The projections were made assuming 13 PAC days of running at 70μA.

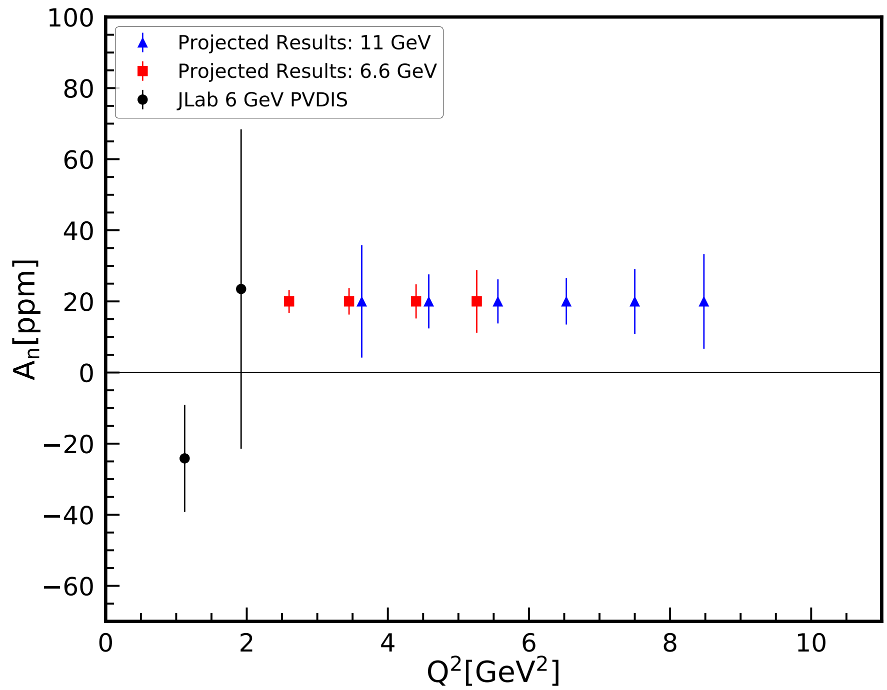

Figure 14: The projected uncertainties on A_n vs. Q^2 from the 6.6 GeV (red) and 11 GeV (blue) beam energy settings of the proposed experiment. A cut of $W > 2$ GeV was applied to select only DIS events. The 6 GeV PVDIS BNSSA data (black) [16] are also shown for comparison.

4 Beam Time Request

We request a total of 38 PAC days of beam time, among which 30 days will be for production running on a 40-cm liquid hydrogen target with a transversely polarized beam of 85% polarization. Among the 38 days, 17 days will be spent at 6.6 GeV and 13 days at 11 GeV. In order to determine the beam polarization, we will require 4 days of dedicated polarimetry measurements, taking into account the additional time needed to rotate the Wien filter angle. The remaining 4 days will be used for commissioning and calibration, including reverse solenoid polarity runs to determine the pair production background. Table 4 summarizes our beam time request.

Purpose	Time (Days)	Energy (GeV)	Beam Current (μA)
Commissioning	2	varies	as needed
Polarimetry	4	varies	as needed
Pass change	0.67	N/A	as N/A
Reverse SoLID polarity	0.67	N/A	N/A
Reverse polarity run	0.33	6.6	70
Reverse polarity run	0.33	11	70
40-cm LH_2 Production	17	6.6	70
40-cm LH_2 Production	13	11	70

Table 4: Beam time request for the proposed experiment.

5 Summary

We propose a high precision measurement of the beam-normal single-spin asymmetry (BNSSA) A_n of the proton in the deep inelastic scattering region. We request a total of 38 PAC days of transversely polarized beam, among which 17 days will be for production at 6.6 GeV and 13 days at 11 GeV, both with a current of 70μA. Additional 4 days are requested for beam polarimetry measurement and 11 days for commissioning, pass change, and calibration, including reverse polarity runs to determine the pair production background. The projected uncertainty on the extracted A_n in the DIS region, if combining all Q^2 bins, is about 2.1 ppm for the 6.6 GeV and 3.8 ppm for the 11 GeV setting. The Q^2 dependence of A_n will be studied by dividing data into Q^2 bins. This will be the first dedicated measurement of BNSSA in DIS to ppm precision. It will test two-photon-exchange (TPE) calculations for BNSSA in DIS. If there exists any effect that amplifies BNSSA predicted by the simple parton-model of TPE, it will be revealed by the proposed measurement.

A Projected Results: Resonance

While not the main focus of this proposal, the SoLID detector would accept a wide range of nucleon resonance scattering event. We investigated the uncertainty of the BNSSA in the resonance region following the same procedure as in the DIS case but now with a $W < 2$ cut. We show in Fig. 15 the ϕ distribution of generated pseudo data at 6.6 GeV and the projected results on A_n in Fig. 16 obtained from the multi-parameter fit. The uncertainty of the resonance A_n extraction from the 11 GeV setting is larger and the details are omitted here.

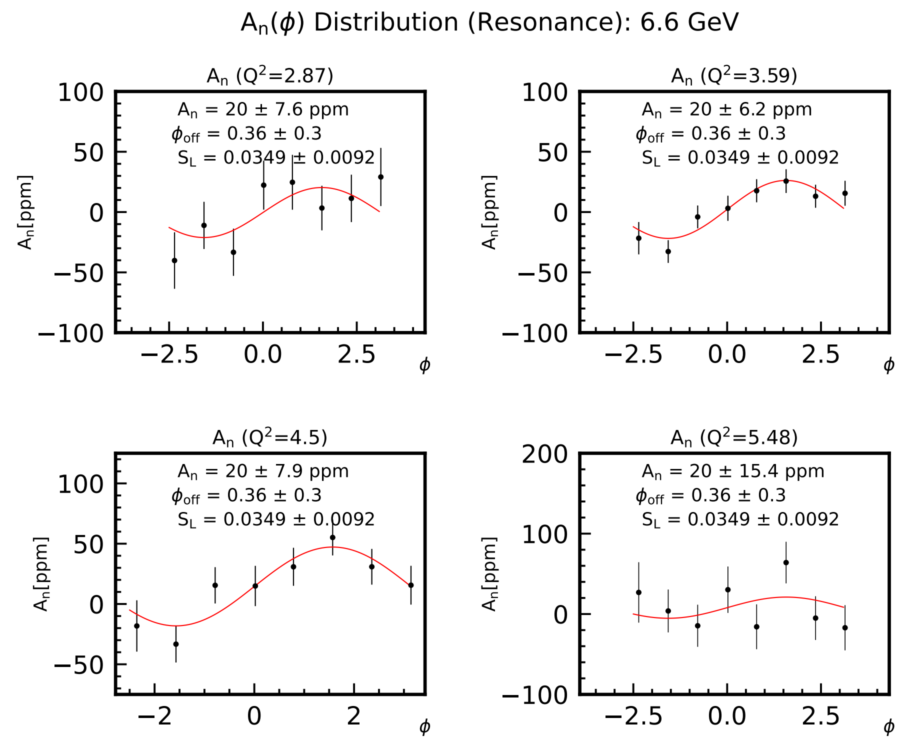

Figure 15: Generated pseudo data for the 6.6 GeV beam energy setting with a $W < 2$ GeV cut to select DIS rates. A common value of the 20 ppm was assumed for the for the size of A_n. The uncertainty in the fitted S_L coefficient was found to be at a level of 0.9%.

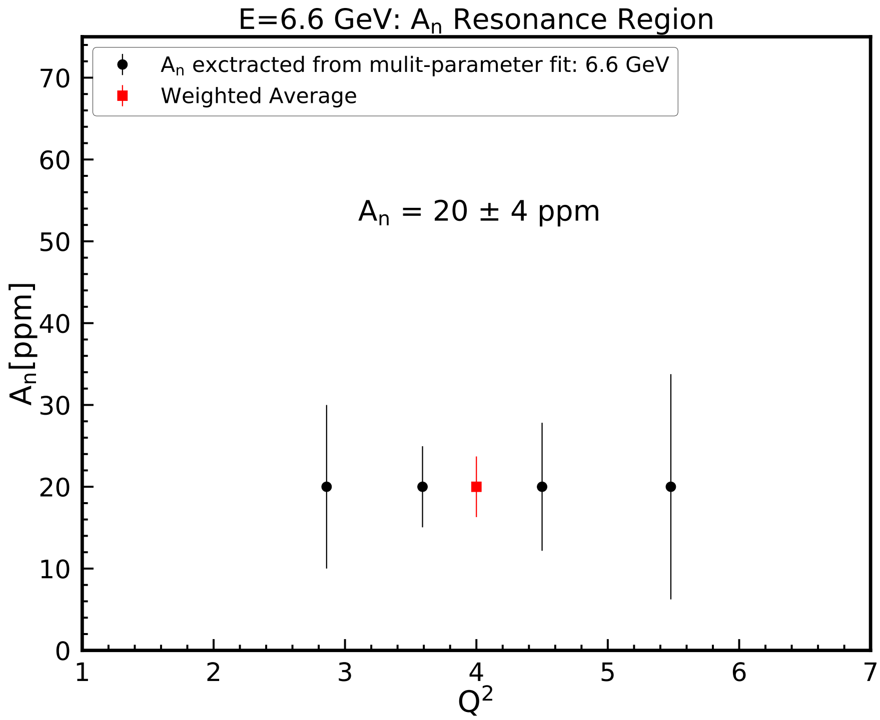

Figure 16: Projected BNSSA along with the weighted average value in the resonance region for 6.6 GeV setting.

Acknowledgment

This work is supported by U.S. Department of Energy under Award number DE–SC0014434.

References

[1] A. J. R. Puckett et al., *Final Analysis of Proton Form Factor Ratio Data at* $\mathbf{Q^2} = \mathbf{4.0}$, *4.8 and 5.6 GeV*$^{\mathbf{2}}$, Phys. Rev. C **85** (2012) 045203, [1102.5737].

[2] M. E. Christy et al., *Form Factors and Two-Photon Exchange in High-Energy Elastic Electron-Proton Scattering*, Phys. Rev. Lett. **128** (2022) 102002, [2103.01842].

[3] I. A. Rachek et al., *Measurement of the two-photon exchange contribution to the elastic* $e^{\pm}p$ *scattering cross sections at the VEPP-3 storage ring*, Phys. Rev. Lett. **114** (2015) 062005, [1411.7372].

[4] CLAS collaboration, D. Rimal et al., *Measurement of two-photon exchange effect by comparing elastic* $e^{\pm}p$ *cross sections*, Phys. Rev. C **95** (2017) 065201, [1603.00315].

[5] OLYMPUS Collaboration collaboration, B. S. Henderson, L. D. Ice, D. Khaneft, C. O'Connor, R. Russell, A. Schmidt et al., *Hard two-photon contribution to elastic lepton-proton scattering determined by the olympus experiment*, Phys. Rev. Lett. **118** (Mar, 2017) 092501.

[6] A. Accardi et al., *An experimental program with high duty-cycle polarized and unpolarized positron beams at Jefferson Lab*, Eur. Phys. J. A **57** (2021) 261, [2007.15081].

[7] J. R. Arrington and M. Yurov, *A measurement of two-photon exchange in Super-Rosenbluth separations with positron beams*, Eur. Phys. J. A **57** (2021) 319, [2103.03752].

[8] A. J. R. Puckett, J. C. Bernauer and A. Schmidt, *Polarization transfer in* $e^{+}p \to e^{+}p$ *scattering using the Super BigBite Spectrometer*, Eur. Phys. J. A **57** (2021) 188, [2104.11879].

[9] E. Cline, J. C. Bernauer and A. Schmidt, *Direct TPE measurement via* $e^{+}p/e^{-}p$ *scattering at low* ε *in Hall A*, Eur. Phys. J. A **57** (2021) 290, [2103.06301].

[10] J. C. Bernauer, V. D. Burkert, E. Cline, A. Schmidt and Y. Sharabian, *Determination of two-photon exchange via* $e^{+}p/e^{-}p$ *Scattering with CLAS12*, Eur. Phys. J. A **57** (2021) 144, [2103.03948].

[11] N. Christ and T. D. Lee, *Possible Tests of Cst and Tst Invariances in l + /- + N –> l + /- + Gamma and A –> B+e++e-*, Phys. Rev. **143** (1966) 1310–1321.

[12] A. Metz, M. Schlegel and K. Goeke, *Transverse single spin asymmetries in inclusive deep-inelastic scattering*, Phys. Lett. B **643** (2006) 319–324, [hep-ph/0610112].

[13] A. Metz, D. Pitonyak, A. Schäfer, M. Schlegel, W. Vogelsang and J. Zhou, *Single-spin asymmetries in inclusive deep inelastic scattering and multiparton correlations in the nucleon*, Phys. Rev. D **86** (Nov, 2012) 094039.

[14] Qweak collaboration, D. Androić et al., *Precision measurement of the weak charge of the proton*, Nature **557** (2018) 207–211, [1905.08283].

[15] PVDIS collaboration, D. Wang et al., *Measurement of parity violation in electron–quark scattering*, Nature **506** (2014) 67–70.

[16] D. Wang et al., *Measurement of Parity-Violating Asymmetry in Electron-Deuteron Inelastic Scattering*, Phys. Rev. C **91** (2015) 045506, [1411.3200].

[17] J. Mar, B. C. Barish, J. Pine, D. H. Coward, H. DeStaebler, J. Litt et al., *Comparison of electron-proton and positron-proton elastic scattering at four-momentum transfers up to 5.0* $(\mathrm{GeV}/c)^2$, Phys. Rev. Lett. **21** (Aug, 1968) 482–484.

[18] B. Gou, J. Arvieux, K. Aulenbacher, D. B. Ríos, S. Baunack, D. Becker et al., *Study of two-photon exchange via the beam transverse single spin asymmetry in electron-proton elastic scattering at forward angles over a wide energy range*, Phys. Rev. Lett. **124** (Mar, 2020) 122003.

[19] QWeak collaboration, D. Androić et al., *Precision Measurement of the Beam-Normal Single-Spin Asymmetry in Forward-Angle Elastic Electron-Proton Scattering*, Phys. Rev. Lett. **125** (2020) 112502, [2006.12435].

[20] QWeak collaboration, D. Androić et al., *Measurement of the Beam-Normal Single-Spin Asymmetry for Elastic Electron Scattering from* ^{12}C *and* ^{27}Al, Phys. Rev. C **104** (2021) 014606, [2103.09758].

[21] F. E. Maas, K. Aulenbacher, S. Baunack, L. Capozza, J. Diefenbach, B. Gläser et al., *Measurement of the transverse beam spin asymmetry in elastic electron-proton scattering and the inelastic contribution to the imaginary part of the two-photon exchange amplitude*, Phys. Rev. Lett. **94** (Mar, 2005) 082001.

[22] Go Collaboration collaboration, D. S. Armstrong, J. Arvieux, R. Asaturyan, T. Averett, S. L. Bailey, G. Batigne et al., *Transverse beam spin asymmetries in forward-angle elastic electron-proton scattering*, Phys. Rev. Lett. **99** (Aug, 2007) 092301.

[23] HAPPEX and PREX Collaborations collaboration, S. Abrahamyan, A. Acha, A. Afanasev, Z. Ahmed, H. Albataineh, K. Aniol et al., *New measurements of the transverse beam asymmetry for elastic electron scattering from selected nuclei*, Phys. Rev. Lett. **109** (Nov, 2012) 192501.

[24] A. Esser, M. Thiel, P. Achenbach, K. Aulenbacher, S. Aulenbacher, S. Baunack et al., *Beam-normal single spin asymmetry in elastic electron scattering off 28si and 90zr*, Physics Letters B **808** (2020) 135664.

[25] A. Afanasev. private communication, 2021.

[26] J. Katich et al., *Measurement of the Target-Normal Single-Spin Asymmetry in Deep-Inelastic Scattering from the Reaction* $^3\mathrm{He}^\uparrow(e,e')X$, Phys. Rev. Lett. **113** (2014) 022502, [1311.0197].

[27] Y. W. Zhang et al., *Measurement of the Target-Normal Single-Spin Asymmetry in Quasielastic Scattering from the Reaction* $^3He^\uparrow(e,e')$, Phys. Rev. Lett. **115** (2015) 172502, [1502.02636].

[28] HERMES collaboration, A. Airapetian et al., *Search for a Two-Photon Exchange Contribution to Inclusive Deep-Inelastic Scattering*, Phys. Lett. B **682** (2010) 351–354, [0907.5369].

[29] A. Averett, H. Yao, A. Camsonne, X. Jiang and N. Liyanage, "Target Single Spin Asymmetry Measurements in the Inclusive Deep-Inelastic Reaction on Transversely Polarized Proton and Neutron (^{3}He) Targets using the SoLID Spectrometer." Jefferson Lab Rungroup Experiment E12-11-108A/E12-10-006A, 2014.

[30] A. O. Barut and C. Fronsdal, *Spin-Orbit Correlations in mu-e and e–e- Scattering*, Phys. Rev. **120** (1960) 1871–1874.

[31] M. Gorchtein, P. A. M. Guichon and M. Vanderhaeghen, *Beam normal spin asymmetry in elastic lepton-nucleon scattering*, Nucl. Phys. A **741** (2004) 234–248, [hep-ph/0404206].

[32] A. Afanasev and M. Vanderhaeghen. private communication, 2022.

[33] A. Afanasev, M. Strikman and C. Weiss, *Transverse target spin asymmetry in inclusive dis with two-photon exchange*, Phys. Rev. D **77** (Jan, 2008) 014028.

[34] O. Koshchii and A. Afanasev, *Target-normal single-spin asymmetry in elastic electron-nucleon scattering*, Phys. Rev. D **98** (2018) 056007, [1803.04004].

[35] P. Souder, "Precision Measurement of Parity-violation in Deep Inelastic Scattering Over a Broad Kinematic Range." Jefferson Lab Experiment E12-10-007, 2010.

[36] J. Benesch. private communication, 2022.

[37] L. Barrón-Palos, a. R. A. others", S. Balascuta, C. Blessinger, J. Bowman, T. Chupp et al., *Determination of the parahydrogen fraction in a liquid hydrogen target using energy-dependent slow neutron transmission*, *Nuclear Instruments and Methods in Physics Research Section A: Accelerators, Spectrometers, Detectors and Associated Equipment* **659** (2011) 579–586.

[38] S. Covrig Dusa. private communication, 2022.

[39] SoLID collaboration, *Solid: Updated preliminary conceptual design report*, https://solid.jlab.org/DocDB/0002/000282/001/solid-precdr-2019Nov.pdf.

[40] P. Adderley, J. Clark, J. Grames, J. Hansknecht, K. Surles-Law, D. Machie et al., *Load-locked dc high voltage gaas photogun with an inverted-geometry ceramic insulator*, *Physical Review Special Topics-Accelerators and Beams* **13** (2010) 010101.

[41] D. Higinbotham. private communication, 2022.

[42] J. Grames. private communication, 2022.

[43] G. Niculescu and I. Niculescu, *The d/p ratio extraction from experiment E12-10-002*, 2021.